

MINERALOGICAL MAGAZINE

VOLUME 61

NUMBER 405

APRIL 1997

Closed system fractionation in a large magma chamber: mineral compositions of the websterite layer and lower mafic succession of the Great Dyke, Zimbabwe

A. H. WILSON AND J. B. CHAUMBA*

Department of Geology and Applied Geology, University of Natal, P.Bag X10, Dalbridge 4014, South Africa

Abstract

The Lower Mafic Succession of the Great Dyke is a 700 m thick sequence of gabbroic rocks which shows remarkably regular mineral compositional trends and trace element contents in whole rocks. Such chemical trends are strongly indicative of undisturbed fractionation having taken place within the magma chamber and contrast with the major development of cyclic units which characterize the underlying Ultramafic Sequence of the Great Dyke. The style of fractionation is quite different to that in the equivalent Main Zone of the Bushveld Complex with the latter possibly reflecting a 'leaky' input system, whereas in the Great Dyke the magma chamber was sealed. Major compositional reversals at the interface between the websterite layer (the topmost unit of the Ultramafic Sequence) and the base of the Lower Mafic Succession indicate a change in crystallization conditions at this level. Modal percentages of plagioclase and Al_2O_3 content of pyroxenes show the same trends indicating a strong control by temperature and magma composition.

Modelling of the fractionation processes and the influence of trapped liquid was carried out for Mg#, Cr_2O_3 , and NiO in pyroxenes and for Zr in whole rock. The lowermost gabbroic rocks are accumulates with effectively zero trapped liquid which contrasts with 10–15% trapped liquid in the underlying websterite. There is a gradual rise in the amount of trapped liquid upwards in the Lower Mafic Succession. These results have implications for the mechanisms by which porosity is reduced in mafic cumulates. An injection of a small amount (10%) of new magma at the interface of the Ultramafic–Mafic Sequences of the Great Dyke was of a composition slightly different to that which gave rise to the cyclic units of the Ultramafic Sequence.

KEYWORDS: Lower Mafic Succession, Great Dyke, Zimbabwe, closed system fractionation, websterite.

Introduction

FRACTIONAL crystallization is a consequence of cooling and crystallization of magma chambers.

The principles are simple and the results are clearly seen in the rocks but the details of process are still not well understood because of the complexity of the processes that take place after initial nucleation of the primary phases. Green (1994) points out that natural mineral assemblages may not always be in compositional equilibrium with each other or the liquid from which these phases formed. Interpretation of

* Present address: Department of Geological Sciences, University of Cape Town, P. Bag Rondebosch, South Africa

compositions must take into account subliquidus reactions with trapped interstitial liquid (Barnes, 1986a; Wilson, 1992) and subsolidus re-equilibration (Wilson, 1982; Hatton and Von Gruenewaldt, 1985) as these obscure the original liquidus compositions. The amount of trapped liquid is controlled by either or both the processes of adcumulus growth (Campbell, 1987) and compaction (McKenzie, 1984; Meurer and Boudreau, 1996).

In addition there are analytical problems associated with re-equilibrated phases and redistribution of components (such as occur by zoning and subsolidus exsolution). Boudreau (1987) also demonstrates the possibility of redistribution of solid phases on the scale of the crystals themselves, or on a micro layer scale. The effect of such processes on minor and trace element contents in minerals and in the whole rock is unknown. Documentation and detailed studies of well characterised rock successions in layered intrusions will ultimately allow such processes to be evaluated and understood in greater detail.

In the light of these complexities the interpretation of liquid composition paths during the evolution of layered intrusions remains enigmatic, even for the Skaergaard intrusion, which is regarded as the classic example of closed system fractionation (Wager, 1960; Hunter and Sparks, 1987, 1990; McBirney and Naslund, 1990; Hanghoj *et al.*, 1995). The driving force for the differentiation of magmas is the continuous separation of crystals to produce a progressively more evolved magma. It is therefore of particular importance to evaluate continuous fractionation trends in large layered intrusions, such as the Great Dyke.

The Great Dyke of Zimbabwe

The Great Dyke is a near-linear intrusive body of mafic and ultramafic rocks cutting across the Archaean craton of Zimbabwe in a NNE direction (Fig. 1). The age of emplacement of the Great Dyke is 2.46 Ga (Hamilton, 1977) and isotopically it has a strong mantle signature. The width varies from 3–11 km and it has a length of 550 km (Wilson and Wilson, 1981). The maximum thickness of the layered succession is 3.25 km (Wilson and Tredoux, 1990) and the strongly flared structure in transverse section was demonstrated by Podmore and Wilson (1987).

The Great Dyke comprises a linear series of narrow, contiguous layered mafic/ultramafic chambers and subchambers which are indicated to have become connected at progressively higher stratigraphic levels (Wilson and Prendergast, 1989) with continued filling and expansion of the magma chamber. Structural re-appraisal of the Great Dyke (Podmore and Wilson, 1987; Prendergast, 1987;

Wilson and Prendergast, 1989) have made it possible to subdivide the Great Dyke into chambers and subchambers (Fig. 1).

Stratigraphically the Great Dyke is divided into a lower Ultramafic Sequence comprising well developed cyclic units of chromitite, dunite and pyroxenite overlain by a succession of gabbroic rocks of the Lower Mafic Succession (LMS) which is the lowermost unit of the Mafic Sequence. The inward-dipping nature of the layering and its axial plunge within each of the subchambers results in rocks of the Mafic Sequence being preserved as isolated occurrences (Fig. 1) along the length of the Great Dyke. The upper part of the Ultramafic Sequence is a websterite and this rock type is of importance because of the extensive development of sulphide mineralization at its base. The sulphide mineralization is in some parts highly enriched in metals of the platinum group of elements giving rise to economically viable ore bodies (Prendergast and Wilson, 1989; Prendergast and Keays, 1989; Wilson and Tredoux, 1990).

Borehole succession studied and methodology

This study encompasses the boundary of the Mafic and Ultramafic Sequences and the lower 600 m of the Lower Mafic Succession in the Sebakwe Subchamber (Fig. 1). Mineral separations (analysed by XRF) were carried out in the grain-size range 0.10–0.18 mm which yields optimum separation of crystals while at the same time preserving the bulk integrity of the exsolved components within the minerals. The separation technique employed the Frantz magnetic separator, heavy liquids and in some cases removal of composite grains by hand picking. In most cases the latter step was not necessary and mineral fractions were determined to be 99.1% to 99.9% pure. For those separates which had a lower degree of purity (i.e. 99.1 to 99.5%) a small correction was made on the basis of the known composition of the contaminating mineral phase. This correction was necessary in about 25% of all separations and was not specific to any one part of the succession. A zone of alteration in the drill core succession, between 12.21 m and 26.7 m above the mafic-ultramafic contact, rendered separation of one or both pyroxenes impossible to the required degree of purity and in such cases the particular mineral was not separated or analysed. The alteration also resulted in highly elevated values of mobile trace elements (Ba, Sr, Rb, K) in the whole rock. Plagioclase separated from this interval was elevated in these elements and minor element compositions for this mineral are unreliable. This alteration is considered to be related to the proximity of a late-stage fault which acted as a passage for fluid migration. In the upper part of the

grains, further complicating the separation process. As a result of these complications clinopyroxene from the upper 95 m of the drill core has been excluded from this study. Nine intervals for close selection of samples were identified so as to examine small within-group variations.

Rock types, textures and modal variations

Websterite layer. The websterite layer (5–36 m thick depending on locality) is the topmost rock unit of the Ultramafic Sequence. The underlying orthopyroxene layer is approximately 200 m thick (Wilson and Wilson, 1981). The lithological importance of the pyroxenite package is due to the presence of sulphide mineralization close to the orthopyroxenite-websterite boundary, part of which is economically enriched in the platinum group elements (Wilson *et al.*, 1989; Prendergast, 1988).

Petrographically the websterite is a medium-grained rock comprising cumulus ortho- and clinopyroxene. Plagioclase is postcumulus and phlogopite, hornblende, opaque minerals and apatite make up the late-stage mineral assemblage. In most occurrences the websterite is relatively homogeneous except for a ubiquitous coarse-grained pegmatoidal pyroxenite 5–30 cm thick immediately underlying the gabbroic contact which has more abundant late-stage minerals.

Lower Mafic Succession (LMS). This is a succession of gabbroic rocks approximately 700 m thick which directly overlies the Ultramafic Sequence. The basal unit is a layered olivine gabbro or olivine gabbro-norite (Wilson and Prendergast, 1989). Olivine occurs as coarse-grained oikocrysts poikilically enclosing plagioclase laths. Large crystals of olivine (1–5 mm) are also found in the upper few centimetres of the websterite layer. Plagioclase, clinopyroxene and orthopyroxene are cumulus phases in the lower part of the succession. Higher up in the succession there is clear evidence of increasing postcumulus overgrowth on cumulus mineral phases by partial enclosure of clinopyroxene by plagioclase laths and inclusions of crystals of ortho- and clinopyroxene in plagioclase. Orthopyroxene oikocrysts up to several centimetres in diameter are found in the top part of the LMS with small individual crystals of inverted pigeonite.

Petrographic evidence is indicative of a marked reduction in postcumulus development in passing from the websterite layer to the basal olivine gabbro. Reappearance of magnesian olivine may be indicative of a new influx of magma but this coincides with the first appearance of plagioclase as a primary liquidus phase which is a totally different situation to that of the lower Ultramafic Sequence where peridotites mark the start of new cyclic units initiated by influx of new magma.

Modal variation. The websterite layer and mafic rocks of the LMS are represented on the modal ternary diagram in Fig. 2. Virtually the entire group of mafic rocks may be classified as gabbro-norites or more specifically clinopyroxene gabbro-norites generally containing more than 60% plagioclase. Most samples from the websterite layer are well within the modal bounds of this rock-type and may be called feldspathic websterites as plagioclase generally exceeds 5% by volume. Several samples immediately below the base of the websterite layer lie on the boundary of the orthopyroxene gabbro but are texturally quite different to those samples in the gabbroic sequence.

In the LMS the main mineral constituents show relatively small overall modal variation (Fig. 3a–c) with the exception of more distinctly felsic layers which may have 10–20% more plagioclase than the normal gabbroic rocks above and below the layer. It is also noticeable that the more feldspar-rich layers have a corresponding lower proportion of clinopyroxene whereas orthopyroxene remains remarkably constant. Minor phases (primary hornblende, phlogopite, opaque minerals and small amounts of quartz) comprise less than 2% by volume, except at the top of the section where there is a noticeable increase in these phases to as much as 8% (Fig. 3d). There is, however, a systematic increase in minor phases upwards in the succession. Considering the average amounts of the various mineral constituents for each of the nine intervals sampled in detail in the LMS, the average content of plagioclase with stratigraphic height shows a systematic decrease from the base of the Mafic Succession (at 63% plagioclase) to the 200 m mark (56% plagioclase) (Fig. 4a). Upwards from this point the volume modal percentage of plagioclase, as an average for each sample group, increases systematically to 65% at the top of the section studied. The large standard deviation for the lowermost group of samples (0–40 m) reflects the strong development of the leuco- and mela-layers, on a centimetre scale, which characterises the base of the LMS. The relative variation of the modal mineral constituents is demonstrated in Fig. 5. The websterite layer shows a strong antipathetic relationship between ortho- and clinopyroxene in the websterites, with a more dispersed but parallel trend exhibited between these two phases in the gabbroic rocks. There is no relationship between modal proportions of orthopyroxene and plagioclase in the mafic rocks and there exists a weak trend of decreasing plagioclase content with increasing amount of orthopyroxene in the websterites. Strong dependence exists between modal percentages of plagioclase and clinopyroxene in the gabbroic rocks and in the websterites. In the gabbroic rocks the trend is one of antipathetic variation and

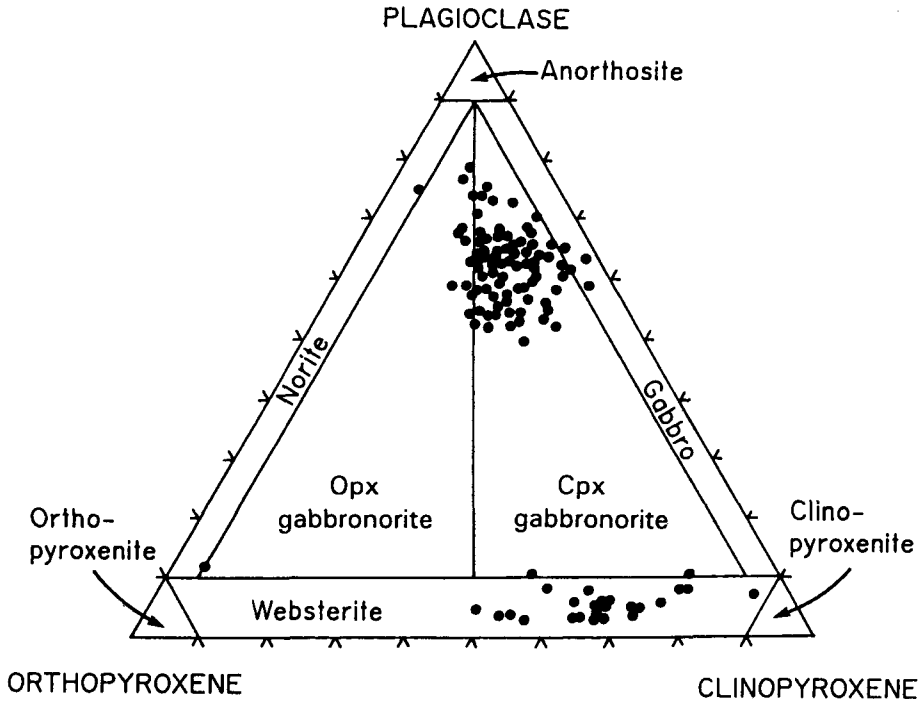


FIG. 2. Modal variation (volume percentage) of rocks of the Lower Mafic Succession and websterite layer considered in this study. The bulk of the mafic rocks lie in the clinopyroxene gabbronorite field. Rocks of the websterite layer are mainly feldspathic websterites.

sympathetic variation in the websterites. These relationships indicate that competition for Ca in the magma may have an influence on the relative proportions of clinopyroxene and plagioclase. The

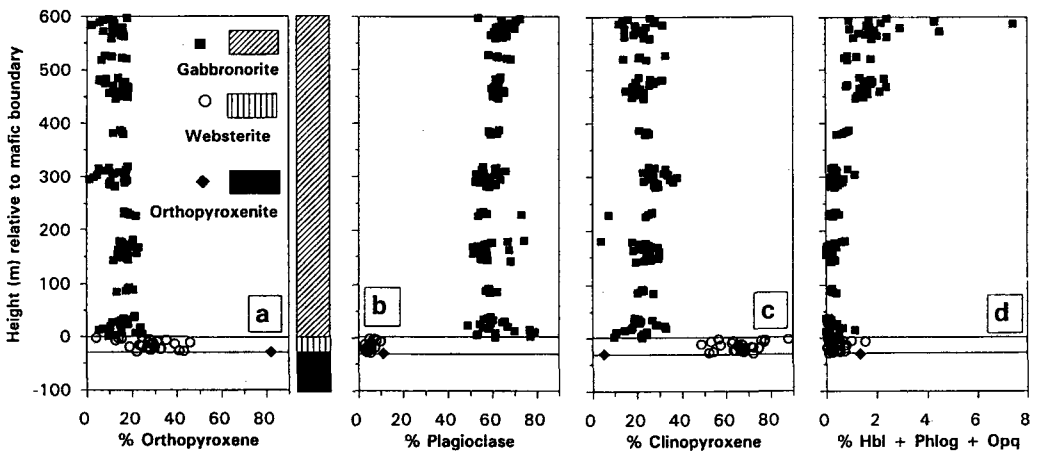


FIG. 3. Modal variations (volume percentage) of minerals (a) orthopyroxene, (b) plagioclase, (c) clinopyroxene, and (d) late stage minerals in rocks of the Lower Mafic Succession and the websterite layer on a stratigraphic basis. The reference line (at 0 metres) is taken at the boundary of these rock units. The lower horizontal line marks the boundary of the websterite layer and the P1 orthopyroxenite.

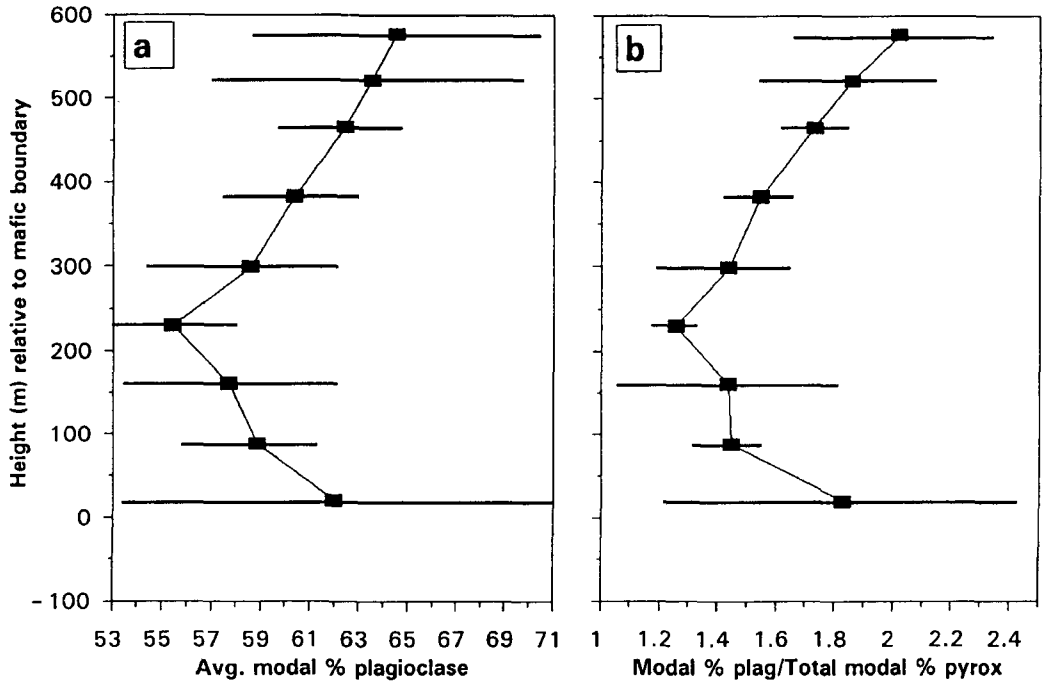


FIG. 4. (a) Average modal variations of plagioclase for each of the nine sample intervals through the Lower Mafic Succession. (b) Averages for each of the nine sample groups for the ratio of modal percent plagioclase to total percent pyroxene. The horizontal bars represent the standard deviation (2 sigma) for each of the sample groups. The very wide range for the lowest group is the result of centimetre-scale modal layering.

same explanation cannot be used for the websterites in which the trend is opposite. In these rocks it would appear that textural rather than chemical controls influence the mineral proportions with the more

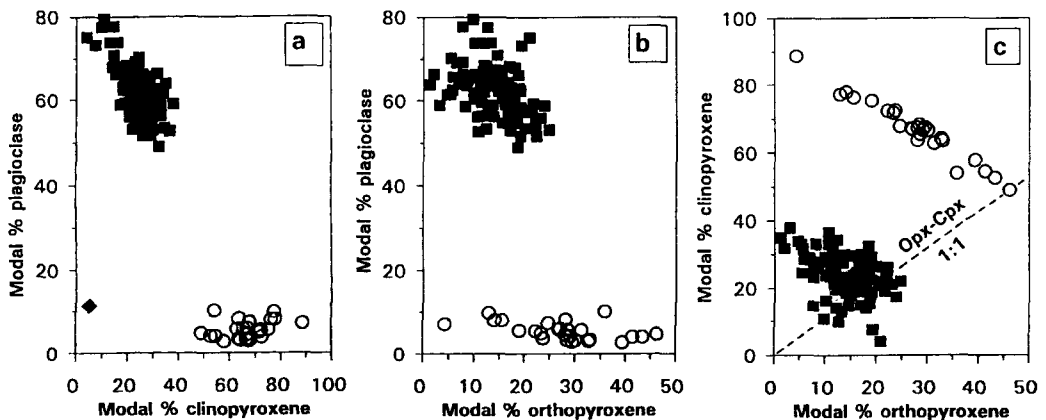


FIG. 5. Binary modal variations for rocks of the Lower Mafic Succession (solid squares), the websterite layer (circles) and orthopyroxenite (solid triangle). (a) Plagioclase versus clinopyroxene. Notice the strong interdependence for the gabbroic rocks. (b) Orthopyroxene versus plagioclase. (c) Clinopyroxene versus orthopyroxene. The 1:1 reference line is shown.

abundant formation of clinopyroxene limiting the available space for the development of early formed postcumulus phases, such as plagioclase.

Whole rock trace element chemistry

Trace elements show highly regular trends through the succession studied and in most cases these highlight the important discontinuity at the websterite-gabbro boundary. The high field strength elements (Zr and Y) (Fig. 6) show a systematic increase upwards through the gabbroic rocks by a factor of more than six. On a stratigraphic basis there is also a major reversal to lower values from the websterites to the lower gabbros with the topmost two samples in the websterites being indistinguishable from the lower gabbros. The upper gabbros lie on the same slightly curved trend as the lower gabbros. Both Zr and Y are significantly enriched in the websterite layer compared with the gabbronorites of the LMS. Y is further enriched in the websterites compared to Zr. The Y content of the websterites is equivalent to that of the mafic rocks some 600 m higher up the sequence. These variations are most easily explained by the websterites having a higher trapped liquid component. The high proportion of clinopyroxene (which has a higher partition coefficient for Y than either plagioclase or orthopyroxene (Rollinson, 1993; Hart and Dunn, 1993)) in the websterites results in further enrichment in this

element. Interpretation of these trends needs to evaluate controls by (a) increasing amount of trapped liquid higher in the succession or, (b) the same amount of trapped liquid but with higher concentrations of incompatible elements resulting from the fractionation process.

Variation in Cu and S reflect sulphide mineralization and both these elements show extreme enrichment in the websterite (Fig. 7) as representing the upper portion of the Main Sulphide Zone (Prendergast and Keays, 1989) but decrease by nearly a factor of 10 in the LMS. In the gabbroic rocks there is a gradual rise in concentration for S but a slight decrease for Cu indicating the development of minor iron sulphide in a system almost entirely depleted in Cu with this element remaining remarkably constant at about 75 ppm. In the plot of Cu vs. S the gabbroic rocks lie on the same trend as the websterites indicating that the system was S saturated but with both these elements highly depleted in the magma as a result of extensive sulphide fractionation in the Main Sulphide Zone.

Pyroxene compositions

Compositions of primary mineral phases provide a quantitative evaluation of the differentiation processes of layered intrusions and have been established in some classic studies of layered intrusions which include Skaergaard (Brown, 1957),

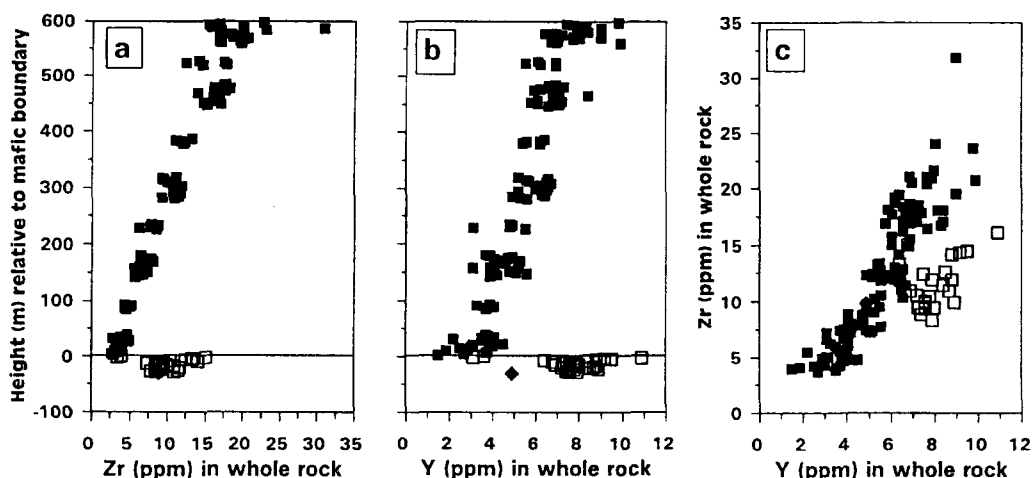


FIG. 6. (a) Stratigraphic variation of Zr in the whole rock showing the major reversal at the boundary of the Lower Mafic Succession and the websterite layer and the gradual increase upwards in the gabbroic rocks. (b) Stratigraphic variation for Y. (c) Mutual dependence between Zr and Y. The websterites do not lie on the same trend as the gabbroic rocks due to the much stronger partitioning of Y into clinopyroxene than into orthopyroxene or plagioclase. Symbols: Solid squares — gabbroic rocks of the Lower Mafic Succession; Open squares — websterite layer; Solid triangle — orthopyroxenite. Reference line (0 metres) is the boundary of the websterite and gabbroic rocks.

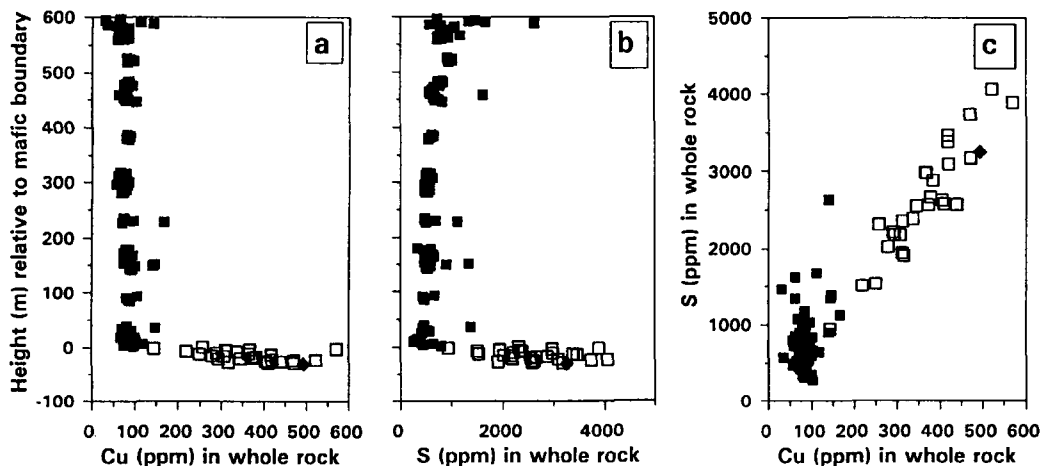


FIG. 7. Variation of (a) Cu, and (b) S through the websterite layer and the Lower Mafic Succession. (c) Mutual variations of Cu and S in whole rocks. Symbols: Solid squares — Lower Mafic Succession; Open squares — websterite layer; Solid triangle — orthopyroxenite.

Bushveld Complex (Atkins, 1969), Jimberlana intrusion (Campbell and Borley, 1974) and Great Dyke (Wilson, 1982). In this study internal analytical consistency of strongly exsolved phases is achieved by carrying out analyses on carefully prepared mineral separates, as well as allowing high analytical precision for large numbers of samples.

A total of 450 mineral analyses were carried out for 150 coexisting assemblages of orthopyroxene, clinopyroxene and plagioclase through the entire sequence studied. Selected analyses are shown in Table 1. The average for the analysis totals for the entire data set is 100.00 ± 0.31 for orthopyroxene and 100.11 ± 0.26 for clinopyroxene. Ferric iron has not been determined but the number of cations for each of the group is very close to the theoretical 4.000 and the charge deficit of close to zero (calculated $(Al^{IV} + Na) - (Al^{VI} + Cr + 2Ti)$) indicates that ferric iron is very low (Cameron and Papike, 1981). A small amount of ferric iron is indicated to be present in the more magnesian pyroxenes in the lower part of the succession studied on the basis of lower charge deficit. This is in keeping with direct analyses for ferric iron in both ortho- and clinopyroxene (Wilson, unpublished data) by which ferric iron decreases upwards in the succession. The data also indicate that the amount of ferric iron in clinopyroxene is approximately three times that in orthopyroxene with the range 0–0.3% in orthopyroxene and 0–0.7% in clinopyroxene. As the emphasis of this study is on an internally consistent data base the calculated values for Fe_2O_3 were not utilized and all iron is assumed to be in the Fe^{2+} state.

Stratigraphic variation in major and minor components in pyroxene

Orthopyroxene. Variation of Mg# (defined as molecular $Mg/(Mg+Fe^{2+})$) and the components Al_2O_3 , CaO, TiO_2 , Cr_2O_3 and NiO in orthopyroxene show highly systematic variation through the sequence (Fig. 8). Mg# decreases upwards in the LMS from 0.84 to 0.55 showing a slightly curvilinear trend. Pyroxenes in the websterite layer have distinctly lower Mg# than for pyroxenes at the base of the Mafic Sequence resulting in a pronounced reversal of compositions across the ultramafic- mafic boundary.

Al_2O_3 content in orthopyroxene overall shows a range from 1.2% to 1.8%. Contiguous samples over intervals of less than 10 m in the section can show a variation of as much as 0.3% which is significantly greater than the determination error of $\pm 0.08\%$ indicating a high degree of small-scale variation. Such small-scale variation is significant but its evaluation is beyond the scope of the present work. The Al_2O_3 contents of orthopyroxene in the websterites are lower but show a gradual increase upwards towards the mafic contact. The pattern for CaO in orthopyroxene shows a marked decrease upwards in the websterite layer with a slight reversal to higher values at the base of the LMS. There is a slight but systematic increase in the CaO content upwards in the succession.

TiO_2 variation in orthopyroxene shows a completely opposite trend to that of Mg# with this component systematically increasing through the

TABLE 1. Representative mineral analyses and trace elements in whole rocks

Pos*	590.0	522.0	522.0	306.0	386.0	386.0	306.0	306.0	156.0	156.0	20.0	20.0	20.00	-4.0	-4.0	-25.0	-25.0	-53.24
Mineral	Opx	Opx	Cpx	Opx	Opx	Cpx	Opx	Opx	Opx	Cpx	Opx	Opx	Cpx	Opx	Cpx	Opx	Opx	Cpx
SiO ₂	52.08	51.92	52.81	54.19	53.33	52.72	54.19	52.77	54.97	53.31	55.72	53.50	53.50	55.23	53.40	55.17	53.24	
Al ₂ O ₃	1.59	1.37	2.41	1.28	1.47	2.20	1.28	2.05	1.30	2.15	1.47	2.57	2.57	1.43	2.24	1.63	2.26	
FeO	22.68	21.96	12.99	17.02	18.40	9.76	17.02	8.85	13.77	7.10	10.27	5.33	5.33	12.71	6.12	11.75	5.92	
MnO	0.50	0.46	0.29	0.36	0.38	0.23	0.36	0.22	0.29	0.19	0.24	0.17	0.17	0.27	0.17	0.25	0.17	
MgO	20.08	20.86	14.09	25.25	23.83	15.19	25.25	16.12	27.50	17.02	30.05	18.10	18.10	28.36	16.93	28.65	17.16	
CaO	2.32	2.14	16.01	1.69	1.89	19.11	1.69	19.26	1.77	19.51	1.80	19.67	19.67	1.89	20.08	1.99	19.84	
Na ₂ O	0.13	0.10	0.67	0.10	0.10	0.45	0.10	0.21	0.12	0.35	0.00	0.29	0.29	0.12	0.31	0.16	0.36	
K ₂ O	0.00	0.00	0.11	0.00	0.00	0.01	0.00	0.02	0.00	0.01	0.00	0.02	0.02	0.18	0.03	0.00	0.02	
TiO ₂	0.328	0.312	0.431	0.228	0.250	0.442	0.228	0.416	0.166	0.279	0.115	0.176	0.176	0.140	0.280	0.124	0.225	
Cr ₂ O ₃	0.007	0.008	0.011	0.012	0.006	0.018	0.012	0.026	0.037	0.080	0.175	0.266	0.266	0.192	0.366	0.368	0.674	
NiO	0.011	0.014	0.009	0.032	0.026	0.017	0.032	0.024	0.044	0.028	0.065	0.051	0.051	0.064	0.042	0.067	0.048	
Total	99.94	99.25	100.08	100.31	99.90	100.33	100.31	100.12	100.08	100.13	99.98	100.21	100.21	100.57	100.31	100.35	100.00	
Site cations on 6 oxygens																		
Si	1.960	1.961	1.974	1.969	1.962	1.953	1.969	1.951	1.971	1.954	1.967	1.944	1.944	1.931	1.954	1.958	1.949	
Al	0.071	0.061	0.106	0.055	0.063	0.096	0.055	0.089	0.055	0.093	0.061	0.110	0.110	0.059	0.097	0.068	0.098	
Ti	0.009	0.009	0.012	0.006	0.007	0.012	0.006	0.012	0.005	0.008	0.003	0.005	0.005	0.004	0.008	0.003	0.006	
Fe	0.714	0.690	0.406	0.517	0.566	0.303	0.517	0.273	0.413	0.218	0.303	0.162	0.162	0.378	0.187	0.348	0.181	
Mn	0.016	0.015	0.009	0.011	0.012	0.007	0.011	0.007	0.009	0.006	0.007	0.005	0.005	0.008	0.005	0.008	0.005	
Mg	1.126	1.174	0.785	1.368	1.307	0.839	1.368	0.888	1.470	0.930	1.581	0.980	0.980	1.502	0.923	1.516	0.936	
Ca	0.094	0.087	0.643	0.066	0.075	0.759	0.066	0.763	0.068	0.766	0.068	0.766	0.766	0.072	0.787	0.076	0.778	
Na	0.009	0.007	0.049	0.007	0.008	0.032	0.007	0.015	0.008	0.025	0.000	0.020	0.020	0.012	0.022	0.010	0.026	
K	0.000	0.000	0.003	0.000	0.000	0.000	0.000	0.001	0.000	0.000	0.000	0.001	0.001	0.000	0.001	0.000	0.001	
Cr	0.000	0.000	0.000	0.000	0.002	0.001	0.000	0.001	0.001	0.002	0.005	0.008	0.008	0.005	0.011	0.010	0.020	
Ni	0.000	0.000	0.000	0.001	0.001	0.001	0.001	0.001	0.001	0.001	0.002	0.002	0.002	0.002	0.001	0.002	0.001	
Mg#	0.612	0.630	0.659	0.726	0.698	0.735	0.726	0.765	0.781	0.810	0.839	0.858	0.858	0.799	0.831	0.813	0.838	
Whole rock trace elements (ppm)																		
Zr	16	18		11	11		11		6		4			13		9		
Y	8	6		6	6		6		4		4			9		8		
Cu	141	96		81	87		81		75		67			313		409		
S	2625	1023		578	653		578		460		-			2350		2574		

* Position in drill core (metres) relative to Mafic-Ultramafic boundary

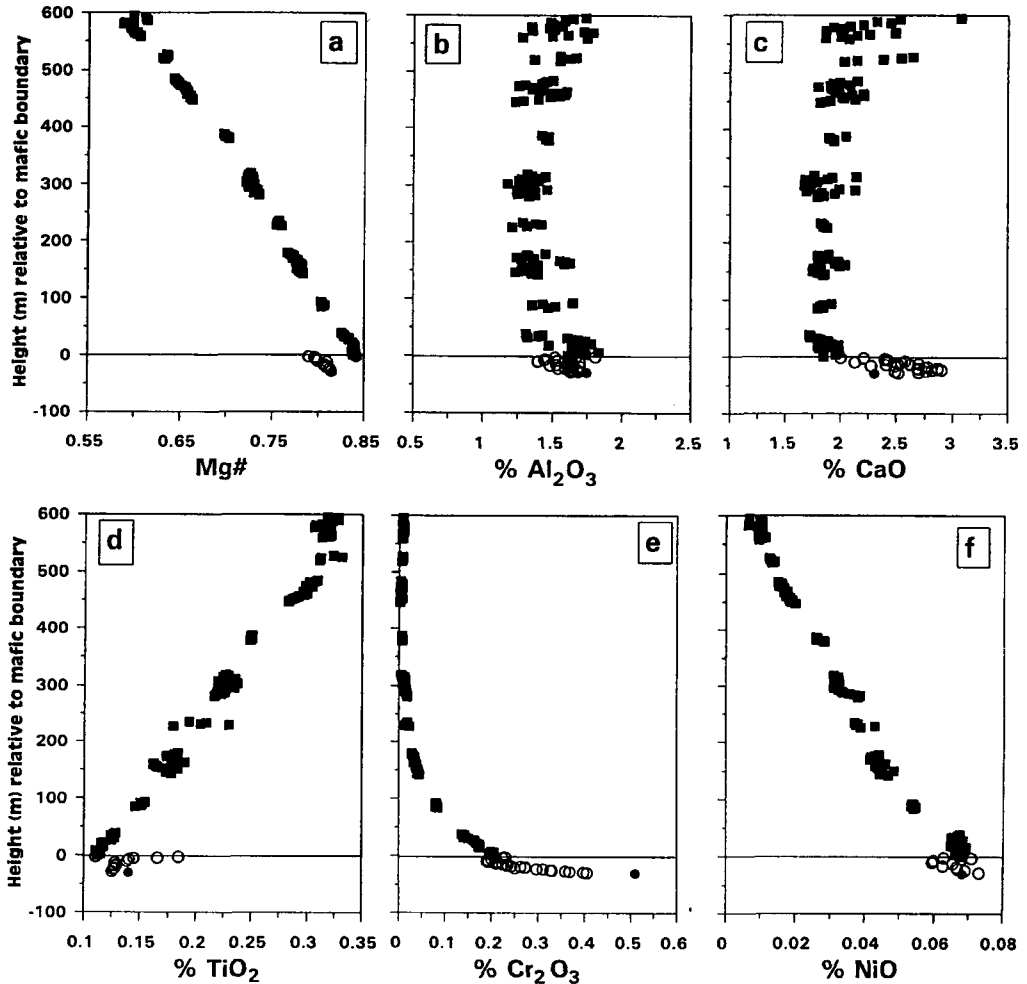


FIG. 8. Stratigraphic variation of major and minor components of orthopyroxene. The reference line marks the boundary of the Lower Mafic Succession (solid squares) and the websterite layer (open circles). Orthopyroxenite is represented by the solid circle. (a) Mg# (as $Mg/(Mg+Fe^{2+})$), (b) Al_2O_3 , (c) CaO, (d) TiO_2 , (e) Cr_2O_3 , (f) NiO.

sequence but with a clear reversal to lower values of TiO_2 at the base the LMS. Variation of Cr_2O_3 through the studied sequence shows a very pronounced trend of upward depletion but continuity of the observed variation and the highly pronounced curve is remarkable. A small reversal to higher values, consistent with all other variables, is observed across the boundary of the websterite layer and the gabbroic rocks. NiO in orthopyroxene shows a systematic decrease upwards in the succession but the rate of decrease is very much less compared with that for Cr_2O_3 . The slightly curvilinear trend is similar to that of Mg#. There is an upward decrease in NiO in the websterite layer with a very pronounced

reversal to higher values in the basal gabbroic rocks.

Clinopyroxene. Very similar trends to those of orthopyroxene are observed for clinopyroxene (Fig. 9). Mg# shows a more pronounced curvilinear trend in clinopyroxene and there is a strong reversal from 0.81 at the top of the websterite layer to 0.86 at the base of the LMS. Al_2O_3 has higher contents in clinopyroxene (2.0–2.7) compared with orthopyroxene but shows the same variation. Calcium in clinopyroxene decreases upwards in the websterite layer but shows a small reversal at the base of the LMS. From 300 m upwards CaO decreases sharply. TiO_2 , Cr_2O_3 and NiO in clinopyroxene show patterns very similar to those of orthopyroxene and all

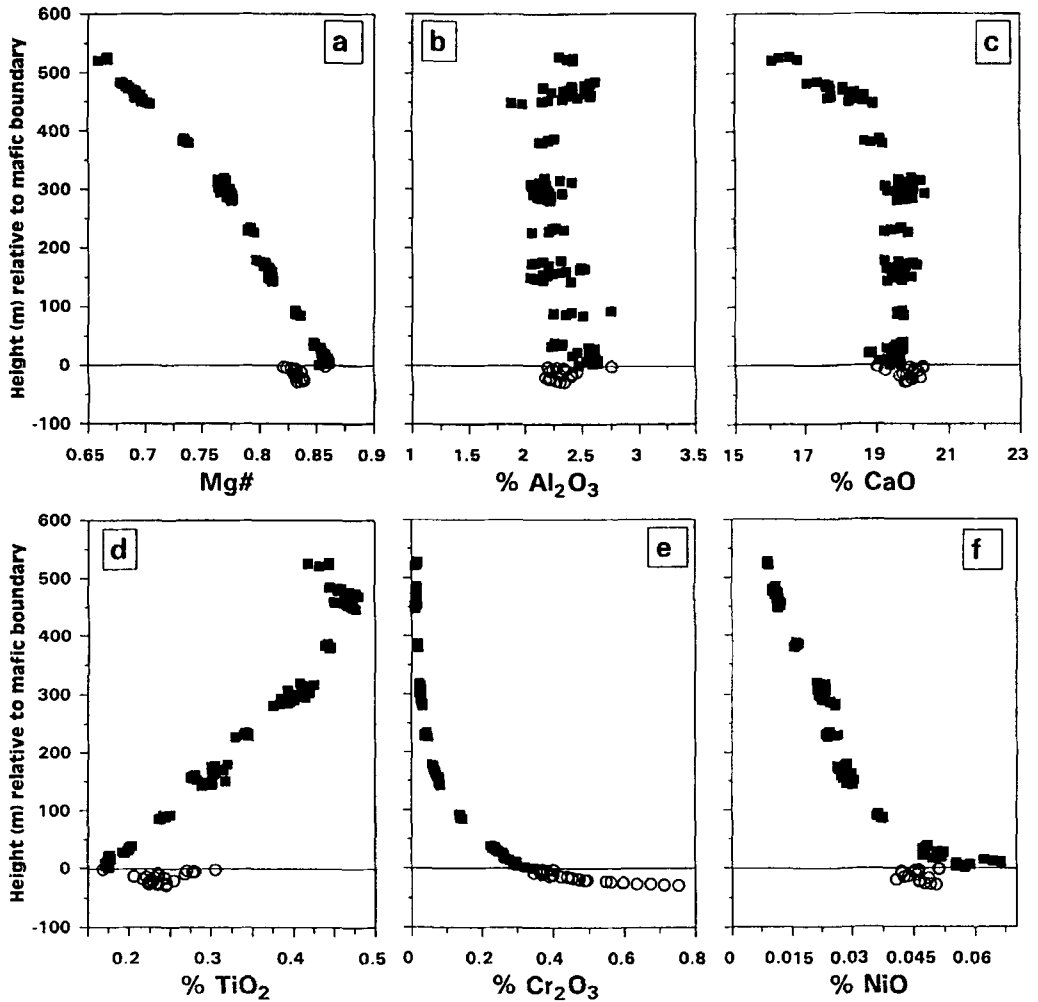


FIG. 9. Stratigraphic variation of major and minor components of clinopyroxene. The reference line marks the boundary of the Lower Mafic Succession (solid squares) and the websterite layer (open circles). (a) Mg# (as $Mg/(Mg+Fe^{2+})$), (b) Al_2O_3 , (c) CaO , (d) TiO_2 , (e) Cr_2O_3 , (f) NiO .

components show a major reversal at the mafic boundary. TiO_2 exhibits a strong decline at the 300 m mark.

Variation of aluminium content of pyroxene

Average values for Al_2O_3 contents, together with standard deviations, for ortho- and clinopyroxene for the stratigraphic section are shown in Fig. 10. The bell-shaped pattern is clear for both pyroxenes and is remarkably similar in form to the variation of modal data through the succession (see Fig. 4). This indicates that the primary magmatic control of the

proportions of crystallizing phases also influenced the aluminium content of the pyroxenes.

Control of Al_2O_3 content in pyroxenes is dependent on both temperature (mainly affecting the octahedral location) and pressure (tetrahedral location) (Mysen and Boettcher, 1975) but with magma composition (silica activity) strongly influencing competition for the tetrahedral site. Considerable small-scale variation in the Al_2O_3 content of pyroxenes from adjacent layers (approximately 0.3%) is similar to the spread of data observed by Eales et al. (1993) for the Bushveld Complex but is not explained by these authors. These

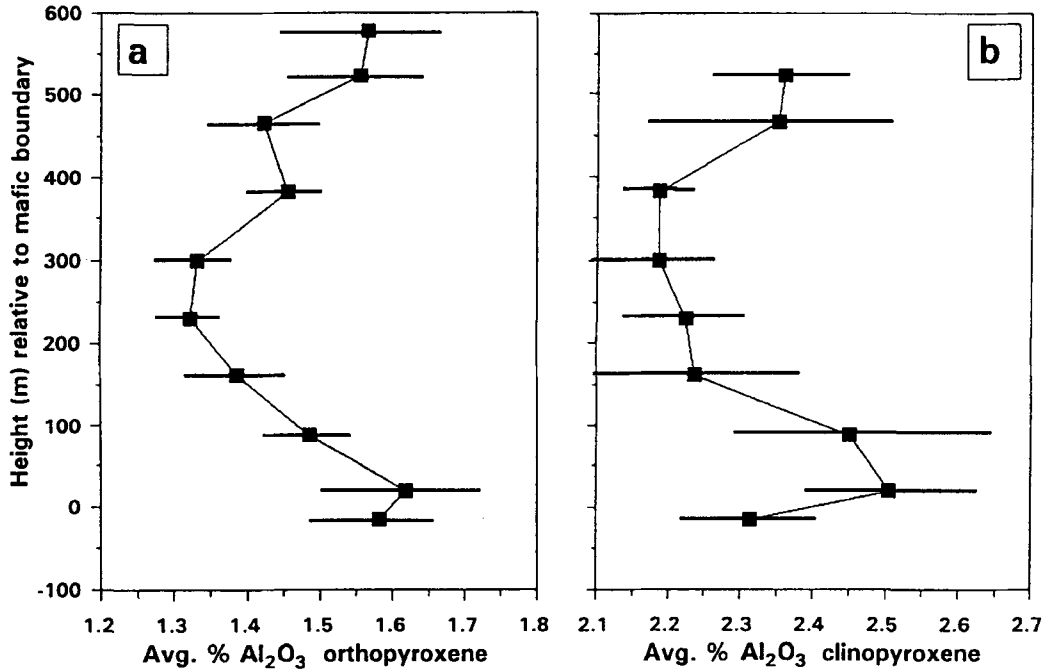


FIG. 10. Average % Al_2O_3 contents for (a) orthopyroxene, and (b) clinopyroxene for each of the nine sample intervals through the Lower Mafic Succession and the websterite layer. The horizontal bars represent the standard deviation (2 sigma) for each of the sample groups.

data indicate small but significant variations in this component which may be related to the dynamics of crystallization of narrow liquid layers within magma chambers. The variation of Al_2O_3 content in orthopyroxene with Mg# has also been expressed as a series of offset linear trends in both the Great Dyke P1 layer (Wilson, 1992) and in the Critical Zone of the Bushveld Complex (Eales *et al.*, 1993).

Stratigraphic variation in major and minor components of plagioclase

Ca# (as $\text{Ca}/(\text{Ca}+\text{Na})$) of plagioclase (Fig. 11a) shows the same systematic variation through the Lower Mafic Sequence as the major components of pyroxene. Values for Ca# decrease from 0.9 at the base of the sequence to 0.72 at the top. A major reversal in composition in plagioclase occurs at the base of the LMS. Plagioclase in the websterite layer is strongly zoned as opposed to the relatively weak zoning observed in the LMS and no systematic compositional trend is observed in the websterite layer.

Variation of K_2O content in plagioclase (Fig. 11b) shows a strongly linear trend (opposite to that for Ca#) with plagioclase directly above the mafic-

ultramafic contact having less than 0.1% K_2O and rising to more than 0.55% at the top of the sequence studied. Again a major reversal occurs for K_2O in plagioclase at the boundary with the mafic rocks with much higher values observed in the websterite layer.

Significance of mineral compositions

The consistency of the patterns observed for the considerable thickness in the LMS of the Great Dyke gives an insight into the fractionation style in this part of the magma chamber. Several important deductions may be made regarding the evolution of the magma chamber: (a) that there is no evidence for injection of magma during the crystallization of the LMS; (b) there is a consistent reversal in all compositional variables between the top of the websterite layer and the base of the LMS; (c) systematic changes in CaO and Al_2O_3 parallel the mineral modal variations and are indicative of an internal control which may reflect changes in magma conditions. The presence of olivine in the basal zone of the LMS is evidence that the transition from the websterite layer to the mafic rocks is not simply the appearance of plagioclase on the liquidus. This break

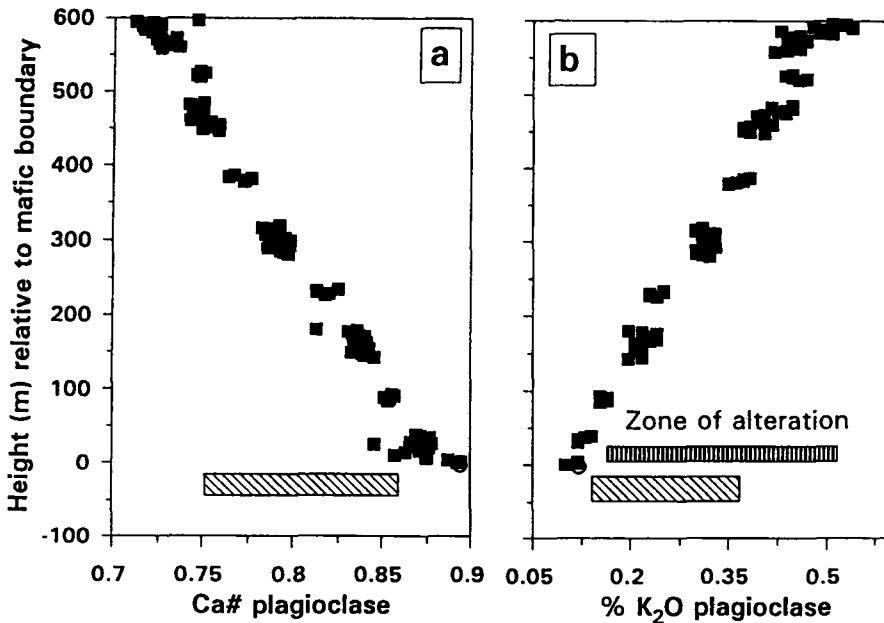


FIG. 11. Stratigraphic variation for plagioclase compositions in the Lower Mafic Succession. (a) Ca# (as Ca/(Ca+Na)), and (b) K₂O content. Lower hashed bar marks the compositional range for the websterite layer. The upper hashed bar in (b) shows a zone of fracture induced alteration where K₂O in plagioclase is disturbed. This alteration does not appear to have affected Ca or Na in plagioclase.

may also be the result of emplacement of new magma which either initiated the crystallization of plagioclase as a primary phase from the pre-existing magma which was saturated with plagioclase, or that this magma was of a different composition and one which was saturated with plagioclase and (at least initially) olivine. In the first case the magma may have been discharged from a chamber at depth which had been undergoing fractionation of Great Dyke type magma.

Comparison of Great Dyke mineral compositions with those of the Main Zone, Bushveld Complex and the Jemberlana Intrusion

The LMS of the Great Dyke may be compared with part of the Main Zone (below the Pyroxenite Marker) and the Upper Critical Zone of the Bushveld Complex where plagioclase becomes a cumulus phase. This Main Zone section is a lithologically continuous succession of norites and gabbro-norites with no interlayered pyroxenites or chromitites and appropriately may be compared with the LMS of the Great Dyke. It is instructive to compare the mineralogical compositions for these two intrusions. Averages of pyroxene compositions (data from

Mitchell, 1990, and unpublished data; Eales *et al.*, 1993; Ashwal, 1995 — for a single analysis of plagioclase for the Lower Critical Zone of the Bushveld Complex) are shown in Fig. 12. Sharpe (1985) argues that the Main Zone of the Bushveld Complex was the product of a single influx of magma whereas Mitchell (1990) suggested that the primocryst mineral compositions supported periods of crystallization interspersed with emplacement of magma. The difference in the rate of change of the various compositional parameters with stratigraphic height between the Great Dyke and the Bushveld Complex is obvious with Mg# for orthopyroxene in the latter changing from 0.74 to 0.60 over 2300 m compared with that in the Great Dyke changing from 0.84 to 0.57 over the much smaller interval of 650 m. The Great Dyke pyroxenes from the LMS are more magnesian than those of the UG-1 Merensky Reef interval and, significantly more so than those at the base of the Main Zone. The variation of Cr₂O₃ in orthopyroxene shows strong depletion but the form of the trend is also different to that of the Great Dyke. Pyroxenes at the base of the Main Zone have lower concentrations of Cr₂O₃ (0.15%) compared to those at the base of the LMS (0.20%). All minor components show a much smaller rate of change in

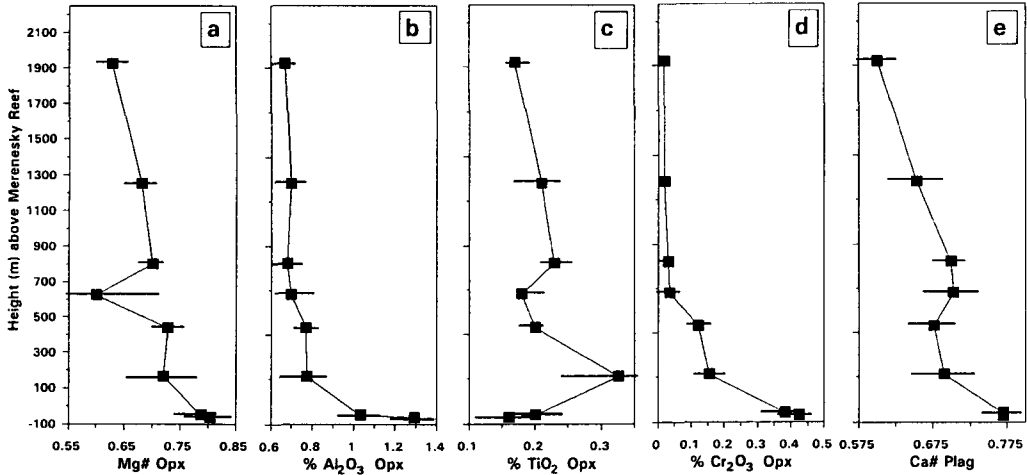


FIG. 12 (a) – (e). Variation of mineral compositional parameters in the Main Zone of the Bushveld Complex. The base of the Main Zone is noted as the 0 metre reference line. Samples below this are in the Upper Critical Zone. The horizontal bars represent standard deviations (2 sigma) for the groups of samples used in the data analysis. Sources of the data are given in the text.

the Bushveld section compared with the Great Dyke. Over this section Cr_2O_3 in orthopyroxene decreases to less than 0.05% at the 700 m mark in the Main Zone whereas this is attained at some 150 m above the mafic-ultramafic contact in the Great Dyke. Al_2O_3 in the Bushveld orthopyroxene is significantly lower compared to the Great Dyke i.e. 0.78 decreasing to 0.67% for the Bushveld Complex compared with 1.8% decreasing to 1.3% for the Great Dyke. Both intrusions show an overall decrease in Al_2O_3 upwards near the base of the gabbroic sequence of rocks. TiO_2 in orthopyroxene is strikingly different in its vertical distribution between the two intrusions. In the Main Zone of the Bushveld Complex this component remains effectively constant over the entire stratigraphic interval at 0.2% in contrast to the dramatic increase observed in the Great Dyke of 0.1 to 0.32%. Eales *et al.* (1993) record a significant increase in TiO_2 in orthopyroxene upwards in the Upper Critical Zone. Ca# for plagioclase (Fig. 12e) for the Main Zone shows relatively low values and a moderate decrease upwards from about 0.72 to 0.60. This is compared with the compositional range of plagioclase in the Great Dyke of 0.90 at the base of the LMS decreasing to 0.72 at the 600 m mark.

This comparison of mineral compositions between the Great Dyke and Bushveld Complex for the same lithological type illustrate not only differences in concentrations of minor components but also their pattern of behaviour in the evolving magma. It also indicates that the primary magma of

the Great Dyke was different to that of the Bushveld Complex, with the former exhibiting initially more primitive compositions for pyroxenes and plagioclase in the lithologically equivalent section. This compositional difference is also likely to have been manifest in correspondingly higher liquidus temperatures for the primary crystallization phases in the Great Dyke gabbroic rocks compared with the Main Zone of the Bushveld Complex. The partitioning of Al_2O_3 and CaO into pyroxene (primarily as the Ca-tschermak component) has been shown by many studies (e.g. Saxena, 1968; Lindsley and Dixon, 1976; Boyd and England, 1964; Fujii, 1976) to be highly temperature dependent resulting in the significantly higher aluminium contents in the Great Dyke pyroxenes. It is also significant that the CaO content (as Wo) is higher in the clinopyroxenes of the Bushveld rocks compared to the Great Dyke, whereas the orthopyroxenes have lower Wo content (Fig. 13). This wider solvus relationship indicates relatively lower temperatures of crystallization in the Bushveld Complex for the same magnesium number of the magma compared with the Great Dyke.

The compositions of the Great Dyke pyroxenes have characteristics which are remarkably similar to those of the Jimberlana Intrusion (Campbell and Borley, 1974). These include the narrower solvus relationships in the pyroxene quadrilateral (Fig. 13) with higher Wo component of orthopyroxene and lower Wo component in clinopyroxene, the steeper slope of clinopyroxene trend in the quadrilateral and

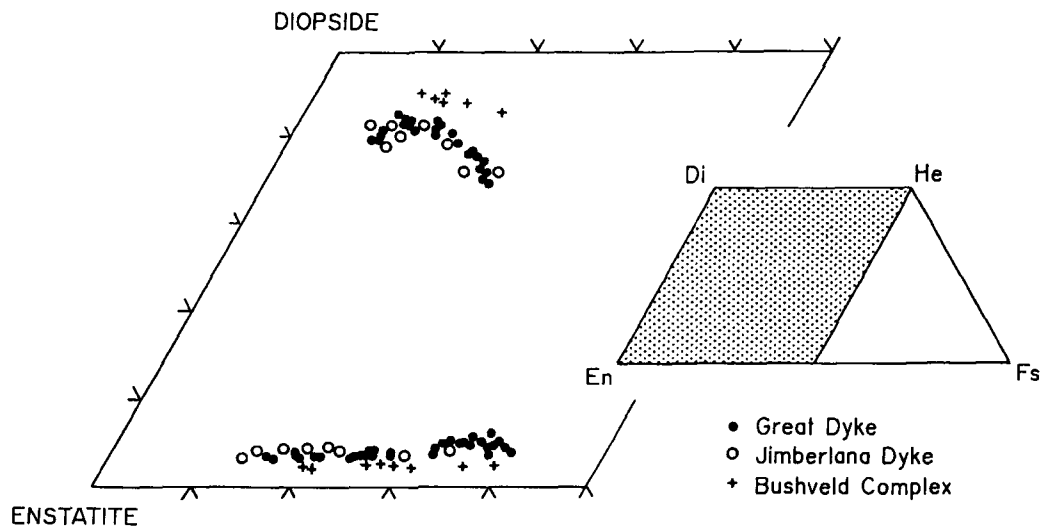


FIG. 13. Projection of ortho- and clinopyroxene compositions of the present Great Dyke study, the Jimberlana Dyke and the Bushveld Complex (Main Zone) into the pyroxene quadrilateral.

the increase in Al_2O_3 content in orthopyroxene at the base of the Gabbroic Zone in that intrusion.

Fractionation modelling for the lower mafic succession

Mineral composition trends in layered intrusions reflect very largely the fractionation sequence in the magma chamber but these may be modified by (a) influxes of magma which may to some extent reset the system, and (b) postliquidus (postcumulus) processes which may modify the original compositions.

The model used here is a computer simulation of sequential fractionation for stoichiometric phase compositions and some trace elements, employing very small finite extractions from the liquid of variable mineral assemblages using established partition coefficients. The trapped liquid component is also an important component causing compositional re-equilibration of liquidus phases to more evolved compositions (as outlined by Barnes (1986a) and Wilson (1992)), as well as the major control of incompatible trace elements in the whole rock. Any realistic modelling requires this factor to be taken into account. Distribution of major (stoichiometric) and trace components between solid and liquid for the various phases is derived from the following sources: FeO/MgO for olivine, orthopyroxene and clinopyroxene — Roeder and Emslie (1970); Beattie *et al.* (1991); Wilson (1992); CaO/Na₂O for plagioclase — Nathan and Van Kirk (1978); Ni in

olivine and the pyroxenes — Barnes (1986b); Beattie *et al.* (1991); Cr in pyroxenes — Barnes (1986a and b); Zr for mafic phases and plagioclase — Rollinson (1993). The partition coefficients of all major components, as well as Ni and Cr, are strongly dependent on liquid composition (as expressed by Beattie (1993) or temperature (as expressed by Barnes (1986b) for Cr in pyroxene). An underlying principle of the model is to take these continuously changing variables into account with the continuous recalculation of liquid compositions thereby changing the partition coefficients.

The fractionation model was run to simulate as closely as possible the modal proportions of primary liquidus phases within the framework of the following parameters: the initial liquid of the Great Dyke (with 15% MgO) and the composition of the liquid at the base of the websterite layer (with 6% MgO) as determined by Wilson (1992); Ni and Cr contents of the liquid at the base of the websterite layer are taken as 300 ppm and 75 ppm respectively (calculated by fractionation of the Ultramafic Sequence of the Great Dyke from the initial liquid); the Zr content of the initial liquid is 64 ppm and is 85 ppm in the liquid at the base of the websterite layer. A further consideration of modelling compositional trends in magma chambers is the relationship of degree of fractionation to relative position within the stratigraphic profile which is dependant on the shape of the magma chamber. In a regularly shaped magma column, fractionation would normally lead to curved compositional trends and therefore matching

of the shape profile would place a constraint on the height – volume relationship.

The results of the modelling of the mineral compositions, trapped interstitial liquid variation and the height-volume profile as derived from optimization of the modelling are shown in Figs. 14–16. Compositional trends show the observed and calculated profiles and represent the closest all round agreement for the various components considered. The amount of trapped interstitial liquid is critical in controlling the distribution of Zr in the whole rock (Fig. 14a). Comparative curves are shown in the geochemical plots for no trapped interstitial liquid and a constant 5% trapped liquid. Consistent with petrographic observations the modelled fractionation indicates that there is a significant reduction of trapped interstitial liquid (Fig. 14b) in passing from the websterite layer (which has up to 15% trapped liquid at the top of the unit) to the base of the LMS (which effectively has no trapped liquid component).

The reduction in trapped interstitial liquid in passing from the websterite layer to the base of the gabbroic rocks would in itself result in a compositional reversal for the cumulus mineral phases with the pyroxenes in the gabbroic rocks being more magnesian. This change would result in a composition shift of 2–3 Mg# units, much lower than the observed reversal of 8 Mg# units. Such a reversal is explained by influx of new magma more primitive than that currently residing in the magma chamber at this level. This new magma may or may not have had

the same composition as the high magnesian primary magma which gave rise to the Ultramafic Sequence of the Great Dyke. An influx of 10–15% new magma would result in the observed reversal of Mg# for pyroxenes (coupled with the change induced by the trapped interstitial liquid as indicated by the variation of Zr content). The height-volume profile in the modelling which overall best fits the shape of the observed chemical trends is shown in Fig. 14c and suggests a narrowing of the magma chamber with increasing height. Modelled compositional variation of Mg# for both orthopyroxene and clinopyroxene (Figs. 15a and 16a) show good agreement with observed trends. Also shown for comparison is the modelled compositional variation where no trapped interstitial liquid is involved. Trapped interstitial liquid has an important effect on the overall fractionation trend. The effect of no trapped interstitial liquid in the gabbroic rocks would lead to a relatively greater rate of iron enrichment in the magma than for the case where a trapped liquid component is involved. The modelled reversal and the overall trend agrees well with observation and an even closer fit would be obtained if a larger input of primary magma was emplaced but this would cause disparity with other chemical trends.

There is very good agreement between observed data and the modelled variation for NiO in pyroxenes (Fig. 15b and 16b) in the websterite layer and for the reversal across the websterite-gabbro boundary. There is also good agreement for the shape of the

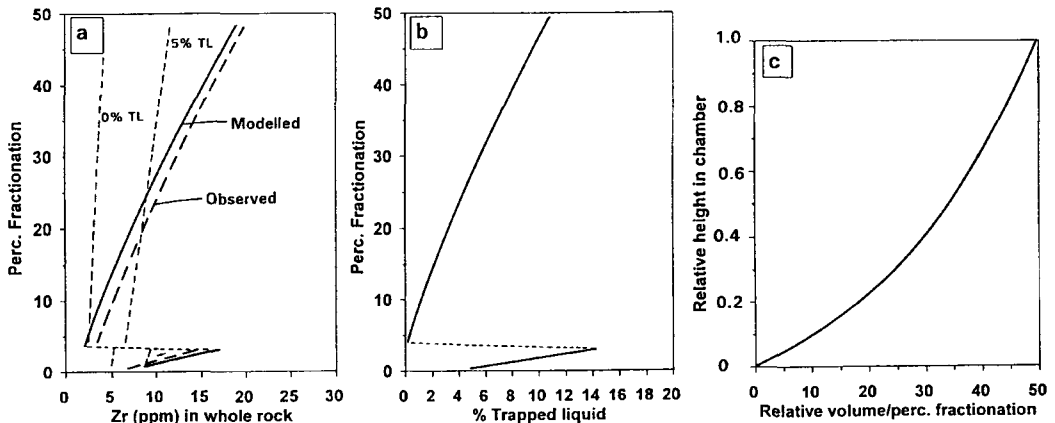


FIG. 14. Results of modelling the fractionation process. (a) Zr in whole rock showing the observed trend and modelled variations encompassing the trapped liquid component. The various curves show the effect of constant 0% and 5% trapped liquid and modelled variable trapped liquid which gives the best agreement with observation. (b) Trapped liquid variation used in the modelled curve of (a). Note the major reversal equating to the boundary of the Lower Mafic Succession and the websterite layer. (c) Curve showing the change of relative volume change upwards in the sequence required to duplicate the curvature of the observed chemical trends. This indicates a narrowing of the magma chamber by some 25% upwards in the succession.

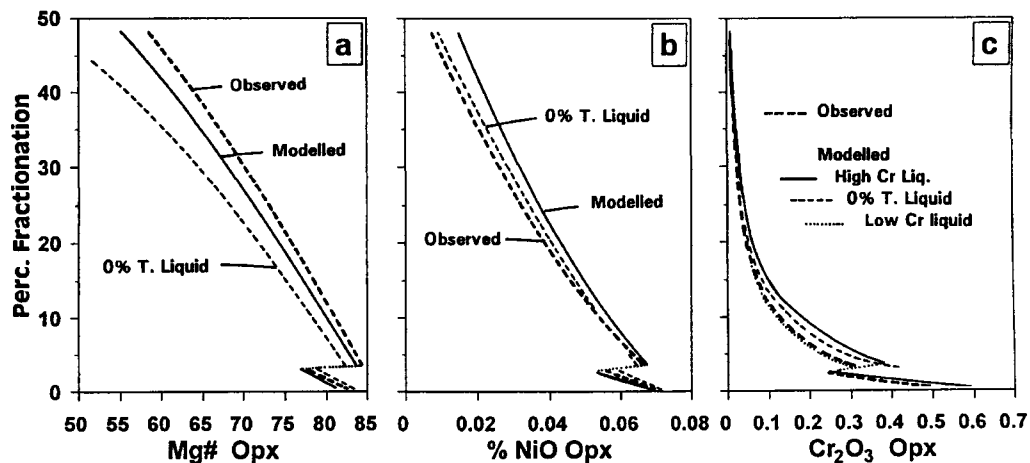


FIG. 15. Comparison of observed trends with results of modelling of the fractionation process for orthopyroxene. (a) Mg#, (b) NiO, (c) Cr₂O₃. The modelled variation takes into account the trapped interstitial liquid component as shown in Fig. 14b. Comparative modelled curves are also shown for 0% trapped liquid.

curve and the NiO content of orthopyroxene in the mafic rocks. However, the observed rate of depletion of NiO in clinopyroxene in the gabbroic rocks is greater than that predicted by the model. This may be an indication of non-equilibration between ortho- and clinopyroxene and this may arise from the difficulty in assessing the cumulus to postcumulus component of the two pyroxenes.

Extreme rate of depletion of Cr₂O₃ is observed for both pyroxenes in the websterite together with a

major reversal at the base of the LMS (Figs. 15c and 16c). The effect of trapped interstitial liquid is minimal because of the very high partition coefficients for this element. The shape of the modelled curve using the accepted composition of Great Dyke magma also agrees well with observation but the degree of reversal, as well as absolute values in the gabbroic rocks, are significantly lower than predicted. It must therefore be deduced that the Cr₂O₃ content of the new influx of magma was lower

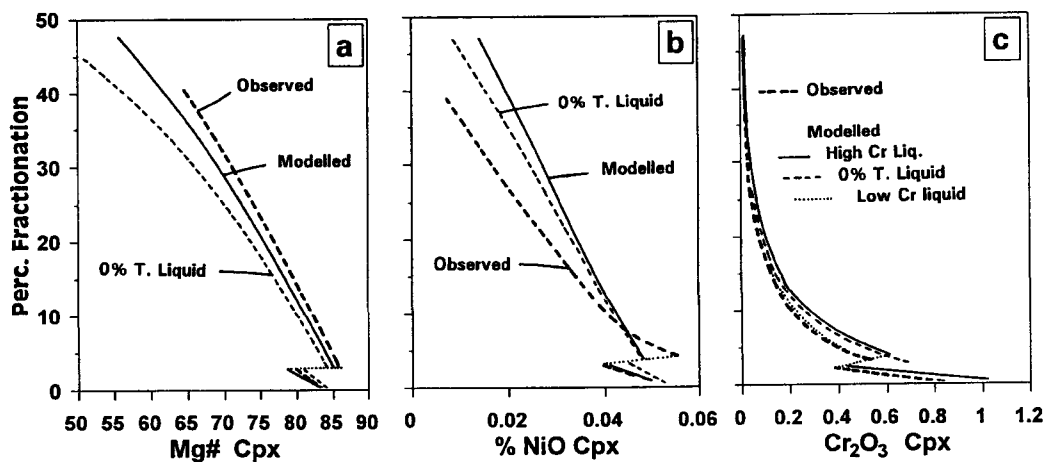


FIG. 16. Comparison of observed trends with results of modelling of the fractionation process for clinopyroxene. (a) Mg#, (b) NiO, (c) Cr₂O₃. The modelled variation takes into account the trapped interstitial liquid component as shown in Fig. 14b. Comparative modelled curves are also shown for 0% trapped liquid.

than that of the magma which gave rise to the Ultramafic Sequence. The modelled profile is shown for influx of magma with 700 ppm Cr rather than that with 1900 ppm Cr as would be appropriate for the primary ultramafic liquid of the Great Dyke. The modelled result for influx of low-Cr magma (Figs. 15c and 16c) shows almost perfect agreement between the observed and modelled trends for both ortho- and clinopyroxene in the LMS.

Discussion

Quantitative evaluation of chemical fractionation in magma chambers is complex and encompasses many processes, some of which act in opposition for some elements and reinforce for other elements as a result of decoupling of the compatible and incompatible elements. In addition to the physical separation of primary phases from the magma, which drives the fractionation process, other important processes include recharge of the chamber by magma which may be of the same or different composition to that which gave rise to the resident magma, and the incorporation of trapped interstitial liquid which influences both the final re-equilibrated composition of the primary mineral phase and the rate at which elements are enriched or depleted in the magma.

Variation of incompatible trace elements allows an estimate of the amount of trapped interstitial liquid arising from the porosity of the solid-liquid assemblage which for mafic cumulates has been variably estimated between zero and as much as 30% (Wager, 1963; Henderson, 1970; Irvine, 1980; Campbell, 1987; Wilson, 1992). Wilson (1992) shows that for the Great Dyke pyroxenites final porosity seldom exceeds 10-15% and this is consistent with the observed variations in the websterite layer in this study. The precise role of secondary (postcumulus) processes in the evolution of mafic rocks, and particularly the mechanisms by which the liquid is eliminated from the crystal mush (generally considered to be by compaction or by primary crystal growth), has long been a source of discussion. Campbell (1987) suggested that the process resulted largely from primary growth mechanisms whereas other arguments favour gravity-driven compaction as being the dominant process (Shierly, 1986; Hunter and McKenzie, 1989; Sparks *et al.*, 1985; Meurer and Boudreau, 1996). Irrespective of which mechanism or combination of mechanisms dominated in establishing the final porosity of the rock the resultant trapped interstitial liquid would have influenced the final compositions of the mineral assemblage and the incompatible element content of the whole rock.

The very low incompatible element content of the basal gabbroic rocks points to these as having

effectively zero porosity. Although this is consistent with the compositional reversal at the mafic boundary it cannot by itself account for the observed compositional change and influx of new magma is a likely possibility. The re-appearance of olivine in the basal mafic rocks supports a disturbance of the system by influx of new magma. However, the coincidence of plagioclase also appearing on the liquidus at this point would suggest that the new magma influx was not of the same composition as the postulated primary magma which gave rise to the Ultramafic Sequence. This is particularly highlighted by the requirement of a much lower Cr content in the new magma compared to that which gave rise to the ultramafic rocks. The origin of such a magma composition is debatable but influx of magmas of different compositions have been proposed to account for the petrogenetic evolution of the Bushveld and Stillwater Complexes (Irvine *et al.*, 1983; Sharpe, 1985; Kruger and Marsh, 1985). There is geophysical evidence of deep-seated magma chambers below the layered series of the Great Dyke and it is possible that fractionated magma from this source may have been emplaced into the Darwendale Subchamber.

Summary and conclusions

(1) Mineral composition trends of the Lower Mafic Zone of the Great Dyke contrast markedly with those observed for an equivalent succession of rock types in the Bushveld Complex both in the concentrations of components and in the evolutionary pattern during fractionation. A significant part of this difference may be that the Bushveld Main Zone represents a 'leaky' input system whereas the magma chamber at this level in the Great Dyke was sealed.

(2) In the Great Dyke the chemical trends for both mineral compositions and incompatible elements in the whole rock show highly regular patterns over wide compositional ranges for the stratigraphic interval studied which allow the quantitative evaluation of the fractionation processes and also an assessment of postcumulus process which may have operated in the formation of these rocks.

(3) The websterite layer has significant amounts of a trapped interstitial liquid component but this never exceeds 15% and for the most part is less than 10%. The basal plagioclase cumulates had very low (approaching zero) trapped interstitial liquid component but it is shown to increase systematically to about 10% at the top of the gabbroic succession. These figures indicate effective exclusion of interstitial liquid from the cumulates. In effect the basal gabbroites of the LMS are adcumulates.

(4) Approximately 50% fractionation in a closed chamber is required to produce the observed mineral

compositions in the 700 m thickness of mafic rocks investigated.

(5) An influx of 10–15% (by mass of resident magma) influx of new magma is required at the websterite–gabbro boundary to explain the compositional reversal as well as the re-appearance of olivine. The composition of this magma must have had significantly lower Cr content than that proposed as the initial magma for the Ultramafic Sequence (i.e. 700 ppm Cr as opposed to 1900 ppm). This suggests that the new magma was mafic and therefore possibly different to the liquid which gave rise to the Ultramafic Sequence. There is no suggestion of either periodic or slow continuous influx of magma taking place during the crystallization of the LMS.

(6) The shapes of the fractionation curves indicate a non-linear relation of magma column width to height with the magma chamber becoming relatively narrower upwards in the succession by about 25%.

(7) Similar patterns for the distribution of Al_2O_3 for both ortho- and clinopyroxenes and the modal percentage of plagioclase in the LMS indicate that both these variables are dependent on the Al activity in the magma. This would in itself depend on many factors, some of which would have been conflictive and others supportive. These factors include the balance of silica and alumina activities, the influence of increased network modifiers at more evolved stages of the magma and decreasing temperature.

Acknowledgements

The Foundation for Research Development (FRD) is acknowledged for supporting this project and providing a postgraduate study bursary to JBC. The University of Natal Research Fund provided financial support for analytical work. Delta Gold Zimbabwe, and in particular Dr D. Gellatly, are thanked for making drill core available for the study. Peter Venderspuy of Delta Gold NL is thanked for his continued support and permission to publish the results of this study. Mr Sam Mawson is thanked for on-site assistance.

References

- Ashwal, L.D. (1995) Trace element geochemistry of Bushveld plagioclase. *Centennial Geocongress Extended Abstracts. Johannesburg: Geological Society of South Africa*, 492–3.
- Atkins, F.B. (1969) Pyroxenes of the Bushveld intrusion, South Africa. *J. Petrol.*, **10**, 222–49.
- Barnes, S.J. (1986a) The effect of trapped liquid crystallization on cumulus mineral compositions in layered intrusions. *Contrib. Mineral. Petrol.*, **93**, 524–31.
- Barnes, S.J. (1986b) The distribution of chromium among orthopyroxene, spinel and silicate liquid at atmospheric pressure. *Geochim. Cosmochim. Acta*, **50**, 1889–909.
- Beattie, P. (1993) Olivine-melt and orthopyroxene-melt equilibria. *Contrib. Mineral. Petrol.*, **115**, 103–11.
- Beattie, P., Ford, C. and Russell, D. (1991) Partition coefficients for olivine-melt and orthopyroxene-melt systems. *Contrib. Mineral. Petrol.*, **109**, 212–24.
- Boudreau, A. E. (1987) Pattern formation during crystallization and the formation of fine-scale layering. In: I. Parsons, (ed.) *Origin of Igneous Layering. NATO ASI Series*. Dordrecht: D. Reidel, 287–312.
- Boyd, F.R. and England, J.L. (1964) The system enstatite-pyrope. *Carnegie Inst. Washington, Ann. Rept. Dir. Geophys. Lab.*, 1963–64, 157–61.
- Brown, G.M. (1957) Pyroxenes from the early and middle stages of fractionation of the Skaergaard intrusion, East Greenland. *Mineral. Mag.*, **31**, 511–43.
- Cameron, M. and Papike, J.J. (1981) Structural and chemical variation in pyroxenes. *Amer. Mineral.*, **66**, 1–50.
- Campbell, I.H. (1987) Distribution of orthocumulate textures in the Jimberlana intrusion. *J. Geol.*, **95**, 35–54.
- Campbell, I.H. and Borley, G.D. (1974) The geochemistry of pyroxenes from the lower layered series of the Jimberlana intrusion, Western Australia. *Contrib. Mineral. Petrol.*, **47**, 281–97.
- Eales, H.V., Teigler, B. and Maier, W.D. (1993) Cryptic variations of minor elements Al, Cr, Ti and Mn in Lower and Critical Zone orthopyroxenes of the western Bushveld Complex. *Mineral. Mag.*, **57**, 257–64.
- Fujii, T. (1976) Solubility of Al_2O_3 in enstatite coexisting with forsterite and spinel. *Carnegie Inst. Washington, Ann. Rept. Dir. Geophys. Lab.*, 1975–76, 566–71.
- Green, T.H. (1994) Experimental studies of trace-element partitioning applicable to igneous petrogenesis - Sedena 16 years later. *Chem. Geol.*, **117**, 1–36.
- Hamilton, J. (1977) Sr isotope and trace element studies of the Great Dyke and Bushveld mafic phase and their relation to early Proterozoic magma genesis in southern Africa. *J. Petrol.*, **18**, 24–52.
- Hanghoj, K., Rosing, M.T. and Brooks, C.K. (1995) Evolution of the Skaergaard magma: evidence from crystallized melt inclusions. *Contrib. Mineral. Petrol.*, **120**, 265–9.
- Hart, S.R. and Dunn, T. (1993) Experimental cpx/melt partitioning of 24 trace elements. *Contrib. Mineral. Petrol.*, **113**, 1–8.
- Hatton, C.J. and von Gruenewaldt, G. (1985) Chromite from the Swartkop Chrome Mine - an estimate of the effects of subsolidus reequilibration. *Econ. Geol.*, **80**, 911–24.

- Henderson, P. (1970) The distribution of phosphorus in the early and middle stages of fractionation of some basic layered intrusions. *Geochim. Cosmochim. Acta*, **32**, 897–911.
- Hunter, R.H. and McKenzie, D.P. (1989) Compaction and textural equilibration in layered intrusions. *28th Int. Geol. Cong., Abstracts*, **2**, 284.
- Hunter, R.H. and Sparks, R.S.J. (1987) The differentiation of the Skaergaard Intrusion. *Contrib. Mineral. Petrol.*, **95**, 451–61.
- Hunter, R.H. and Sparks, R.S.J. (1990) The differentiation of the Skaergaard Intrusion: a discussion. *Contrib. Mineral. Petrol.*, **104**, 248–54.
- Irvine, T.N. (1980) Magmatic infiltration metasomatism, double diffusive fractional crystallization and adcumulus growth in the Muskox intrusion and other layered intrusions. In: R.B. Hargraves, (ed.) *Physics of Magmatic Processes*. Princeton: Princeton Univ., 325–83.
- Irvine, T.N., Keith, D.W. and Todd, S.G. (1983) The J-M platinum-palladium reef of the Stillwater Complex, Montana: II. Origin by double-diffusive convective magma mixing and implications for the Bushveld Complex. *Econ. Geol.*, **78**, 1287–334.
- Kruger, F.J. and Marsh, J.S. (1985) Significance of Sr87/Sr86 ratios in the Merensky cyclic unit of the Bushveld Complex. *Nature*, **298**, 53–55.
- Lindsley, D.H. and Dixon, S.A. (1976) Diopside-annite equilibria at 850°C to 1400°C, 5 to 35 kb. *Amer. J. Sci.*, **276**, 1285–301.
- McBirney, A.R. and Naslund, H.L. (1990) The differentiation of the Skaergaard Intrusion: a discussion. *Contrib. Mineral. Petrol.*, **104**, 235–40.
- Meurer, W.P. and Boudreau, A.E. (1996) Compaction of density-stratified cumulates: effect on trapped-liquid distribution. *J. Geol.*, **104**, 115–20.
- McKenzie, D.P. (1984) The generation and compaction of partially molten rock. *J. Geol.*, **25**, 713–65.
- Mitchell, A.A. (1990) The stratigraphy and mineralogy of the Main Zone of the northwestern Bushveld Complex. *S. Afr. J. Geol.*, **93**, 818–31.
- Mysen, B.O. and Boettcher, A.L. (1975). Melting of hydrous mantle: II. Geochemistry of crystals and liquids by anatexis of mantle peridotite at high pressures and high temperatures as a function of controlled activities of water, hydrogen and carbon dioxide. *J. Petrol.*, **16**, 549–93.
- Nathan, H.D. and Van Kirk, C.K. (1978) A modal of magmatic crystallization. *J. Petrol.*, **19**, 66–94.
- Podmore, F. and Wilson, A.H. (1987) A reappraisal of the structure, geology and emplacement of the Great Dyke, Zimbabwe. In: H.C. Halls & W.F. Fahrig, (eds.) *Mafic Dyke Swarms*. *Geol. Assoc. Canada Spec. Paper* **34**, 317–30.
- Prendergast, M.D. (1987) The chromite ore field of the Great Dyke, Zimbabwe. In: C.W. Stowe, (ed.) *Evolution of Chromium Ore Fields*. New York: Van Nostrand Reinhold, 89–108.
- Prendergast, M.D. (1988) The geology and economic potential of the PGE rich Main Sulphide Zone of the Great Dyke, Zimbabwe. In: H.M. Pritchard, P.J. Potts, J.F.W. Bowles and S.J. Cribb, (eds.) *Geo-Platinum 87*. London: Elsevier, 281–302.
- Prendergast, M.D. and Keays, R.R. (1989) Controls of platinum-group element mineralization of the PGE-rich Main Sulphide Zone in the Wedza Subchamber of the Great Dyke, Zimbabwe: implications for the genesis of, and exploration for, stratiform PGE mineralization in layered intrusions. In: M.D. Prendergast and M. Jones, (eds.) *5th Magmatic Sulphides Field Conference, Harare, Zimbabwe*. London: Institution of Mining and Metallurgy, 43–69.
- Prendergast, M.D. and Wilson, A.H. (1989) The Great Dyke of Zimbabwe. II Mineralization and mineral deposits. In: M.D. Prendergast and M. Jones, (eds.) *5th Magmatic Sulphides Field Conference, Harare, Zimbabwe*. London: Institution of Mining and Metallurgy, 21–42.
- Roeder, P.L. and Emslie, R.F. (1970) Olivine-liquid melt equilibrium. *Contrib. Mineral. Petrol.*, **29**, 275–89.
- Rollinson, H. (1993) *Using geochemical data: Evaluation, Presentation, Interpretation*. New York: Longman Scientific and Technical. 352 pp.
- Saxena, S.K. (1968) Distribution of elements between coexisting minerals and the nature of solution in garnet. *Amer. Mineral.*, **53**, 994–1014.
- Sharpe, M.R. (1985) Strontium isotopic evidence for preserved density stratification from the Main Zone of the Bushveld Complex, South Africa. *Nature*, **316**, 119–26.
- Shirley, D.N. (1986) Compaction of igneous cumulates. *J. Geol.*, **94**, 795–809.
- Sparks, R.S.J., Huppert, H.E, Kerr, R.C., McKenzie, D.P. and Tait, S.R. (1985) Postcumulus processes in layered intrusions. *Geol. Mag.*, **122**, 555–68.
- Wager, L.R. (1960) The major element variation of the layered series of the Skaergaard intrusion and a re-estimation of the average compositions of the hidden layered series and of the successive residual magmas. *J. Petrol.*, **1**, 364–98.
- Wager, L.R. (1963) The mechanism of adcumulus growth in the layered series of the Skaergaard intrusion. *Mineral. Soc. Amer. Spec. Paper*, **1**, 1–19.
- Wilson, A.H. (1982) The geology of the Great Dyke, Zimbabwe: The ultramafic rocks. *J. Petrol.*, **23**, 240–92.
- Wilson, A.H. (1992) The geology of the Great Dyke, Zimbabwe: Crystallization, layering, and cumulate formation in the P1 pyroxenite of Cyclic Unit 1 of the Darwendale Subchamber. *J. Petrol.*, **33**, 611–663.
- Wilson, A.H. and Prendergast, M.D. (1989) The Great

- Dyke of Zimbabwe. I: Tectonic setting, stratigraphy, petrology, structure, emplacement and crystallization. In: M.D. Prendergast and M. Jones, (eds.) *5th Magmatic Sulphides Field Conference, Harare, Zimbabwe*. London: Institution of Mining and Metallurgy, 1–20.
- Wilson, A.H. and Tredoux, M. (1990) Lateral and vertical distribution of the platinum-group elements and petrogenetic controls on the sulfide mineralization in the P1 pyroxenite layer of the Darwendale Subchamber of the Great Dyke, Zimbabwe. *Econ. Geol.*, **85**, 556–84.
- Wilson, A.H. and Wilson, J.F. (1981) The Great 'Dyke'. In: D.R. Hunter, (ed.) *Precambrian of the Southern Hemisphere*. Amsterdam: Elsevier, 572–8.
- Wilson, A.H., Naldrett, A.J. and Tredoux, M. (1989) Distribution and controls of platinum-group element and base metal mineralization in the Darwendale Subchamber of the Great Dyke, Zimbabwe. *Geology*, **17**, 649–52.

[Manuscript received 29 February 1996:
revised 23 September 1996]